

# Development of a Heat Exchanger with Integrated Thermal Storage for Spacecraft Thermal Management Applications

Kuan-Lin Lee<sup>1</sup>, Calin Tarau<sup>2\*</sup>, and Nathan Van Velson<sup>3</sup>  
*Advanced Cooling Technologies, Inc., Lancaster, PA, 17601*

In order to reduce the mass of on-board thermal management systems for NASA future space missions, Advanced Cooling Technologies, Inc. (ACT) has developed an innovative heat exchanger that integrates phase change material (PCM) within a vapor chamber. The developed PCM-based heat exchanger consists of multiple ultra-thin aluminum drawers charged with bulk PCM ( $T_m \sim 25^\circ\text{C}$ ). The exterior of each drawer was wrapped with screen mesh, which serves as the wick structure to transport the working fluid (acetone) back to the heated regions. Depending on the sink temperature, the developed device can either function as a thermal capacitor or a two-phase heat exchanger with thermal storage capability. During the spacecraft launching stage, the excessive heat carried via the saturated vapor will be stored within the PCM and then released back to the two phase medium and further out of the heat exchanger during the orbiting stage. The aluminum-acetone heat exchanger with multiple drawers can potentially achieve a high PCM/total mass ratio ( $\sim 0.7$ ). This paper reports on the development of the PCM-based heat exchanger, including conceptual designs, analytical modeling, prototype fabrication and the experimental system.

## Nomenclature

$A_m$	=	Area of screen mesh
$A_{evap}$	=	Evaporation heat transfer area
$k_l$	=	Liquid PCM thermal conductivity
$k_f$	=	Working fluid thermal conductivity
$k_m$	=	Mesh wire thermal conductivity
$k_{eff}$	=	Effective thermal conductivity of the saturated mesh
$m_{pcm}$	=	Mass of PCM
$m_{total}$	=	Mass of total system
$M_R$	=	System mass ratio
$q''$	=	Heat flux coming from the evaporator
$q_{in}$	=	Heat flux into the PCM drawer
$R$	=	Thermal Resistance
$T_m$	=	Melting Temperature of PCM
$T_l$	=	Liquid PCM temperature
$t_m$	=	Mesh wire thickness
$\delta$	=	PCM melting region thickness
$\varepsilon_m$	=	Screen mesh porosity
$\lambda$	=	Working fluid latent heat of vaporization
$\lambda_f$	=	PCM latent heat of fusion
$\mu$	=	Working fluid viscosity
$\rho_l$	=	Working fluid liquid density
$\rho_v$	=	Working fluid vapor density
$\rho_{pcm}$	=	Liquid PCM density

<sup>1</sup> R&D Engineer, Defense & Aerospace Products Group, 1046 New Holland Ave.

<sup>2</sup> Lead Engineer, Defense & Aerospace Products Group, 1046 New Holland Ave.

<sup>3</sup> R&D Engineer, Defense & Aerospace Products Group, 1046 New Holland Ave.

## I. Introduction

Due to the large latent heat of fusion, phase change materials (PCM) can store a large amount of energy within a small volume, making them ideal for spacecraft thermal management applications. Typical PCM-based heat exchangers are embedded with a solid heat transfer structure, such as aluminum fins or foam or even carbon foam to enhance the overall thermal conductance. These additional solid structures typically consume around 50% of the system mass, making it very difficult to achieve a high mass ratio ( $M_R$ ), which is defined as

$$M_R \equiv \frac{m_{pcm}}{m_{total}}$$

For spacecraft thermal management applications, it is essential to reduce the overall mass of on-board thermal storage system and minimize the temperature fluctuation when the environmental temperature changes dramatically. Under a Small Business Innovation Research (SBIR) Program from NASA Marshall Space Flight Center (MSFC), Advanced Cooling Technologies, Inc. (ACT) has developed several innovative heat exchangers with thermal storage capability that integrate PCM into vapor chambers. By replacing the solid heat transfer medium with the two-phase working fluid, both overall mass of the developed thermal storage module and thermal resistance can be reduced significantly. Under the program, two different heat exchanger concepts were examined. The first heat exchanger incorporates microencapsulated PCM beads which can serve as thermal storage medium as well as the wick structure for working fluid transportation<sup>1</sup>. The second PCM-based heat exchanger concept integrates multiple rectangular drawers loaded with bulk PCM into a vapor chamber. In this design, PCM enclosed inside the metallic drawers still serves as the thermal storage medium but the working fluid transportation is handled by a wick structure (i.e. screen) attached to the exterior surface of the drawers. This paper is focused on the development of the second design, including the basic concept, design methodologies, theoretical analysis, prototype fabrication and preliminary test results.

## II. Heat Exchanger with PCM Drawers

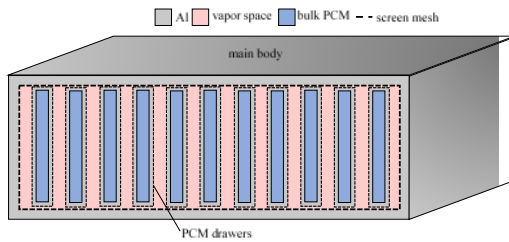


Figure 1. PCM heat exchanger concept

The developed heat exchanger is shown in Figure 1. It consists of a main body and multiple rectangular envelopes filled with bulk PCM, which are named as the “PCM drawers”. For the purpose of liquid return, the exterior surface of the drawers and the interior surface of the main body are wrapped with metallic screen mesh. The shift in the design concept from using micro-encapsulated PCM beads to using bulk PCM enclosed within individual drawers is due to concerns with the structural integrity of the encapsulated beads, and non-condensable gas generation that was occurring during intensive testing of the micro-PCM. The developed heat exchanger has two different modes of

operation, which are depicted in Figure 2. When the environmental temperature is lower than the PCM melting temperature, the device operates in the heat exchanger mode, which is very similar to a standard vapor chamber. Heat applied on one surface (evaporator) of the device will vaporize the working fluid. The saturated vapor quickly spreads and occupies the entire volume of the vapor space. Heat is removed on the other surface (condenser) where vapor is condensed back into liquid. The condensed liquid is then driven back to the heating surface through the capillary pressure of the wick structure (e.g. mesh screen). The saturated vapor can transfer heat more effectively and more uniformly than the pure conduction. When the environmental temperature is higher than the melting temperature of

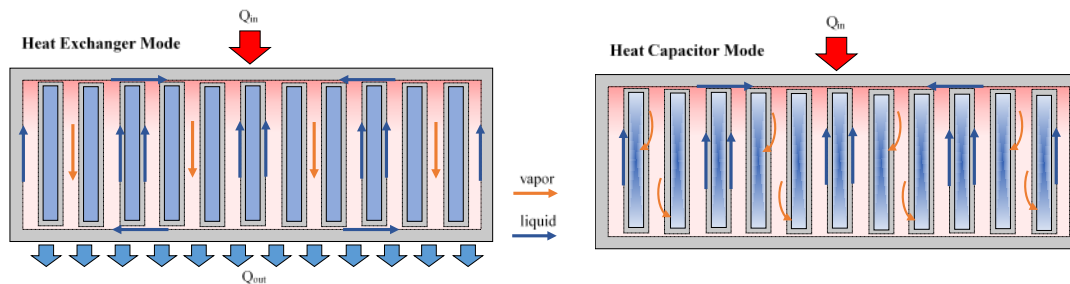


Figure 2. PCM heat exchanger different modes of operation

the PCM, or no heat is able to be dissipated at the condenser surface (for example: during the launch stage of a spacecraft), the device operates in a heat capacitor mode. The saturated vapor will condense on the PCM drawer's surface and release the latent heat into bulk PCM. PCM will keep storing heat in the form of latent heat of fusion until the sink temperature drops below the melting point of the PCM, e.g. at the orbit stage. The heat stored within PCM will then be released into the heat exchanger and the device will go back to the normal heat exchanger mode. Several advantages of the drawer design can be summarized as follows:

- By replacing the solid heat transfer material with a two-phase working fluid, the system mass can be reduced significantly.
- Using aluminum as the structural material can potentially achieve a high system mass ratio. ( $>2/3$ )
- The device can function as a heat capacitor as well as a heat spreader. Therefore, it can eliminate the need for two separate devices in space thermal management systems.
- No moving parts are involved in the system, making it extremely reliable for long-term flight missions.
- The PCM drawers provide the additional structural support, preventing the heat exchanger from collapsing.
- The system can be low cost and relatively easy to fabricate.

### III. Design Method and Theoretical Analysis

#### A. Material, Working Fluid and Wick Structure

To minimize the mass of the structure material, the heat exchanger main body and the drawer envelope were made by aluminum. Acetone was selected as the most compatible working fluid for this system. The properties comparison between acetone and methanol (Table 1) shows that acetone has comparable two-phase heat transport capability to a common heat pipe working fluid. The wicking capability of the aluminum mesh and the acetone was tested by vertically inserting the aluminum screen mesh into a graduated cylinder with dyed acetone. Results show that acetone can wick approximately 4.45 cm (1.75") up the aluminum screen, which indicates that the static contact angle of acetone on aluminum mesh is about 55°.

**Table 1. Thermal and fluid properties of methanol and acetone at T=40°C**

	Methanol	Acetone
Vapor pressure (Pa)	$3.343 \times 10^4$	$6.0 \times 10^4$
Liquid density (kg/m <sup>3</sup> )	779.552	768
Vapor density (kg/m <sup>3</sup> )	0.448	1.05
Liquid viscosity (kg/m s)	$4.436 \times 10^{-4}$	$2.69 \times 10^{-4}$
Vapor viscosity (kg/m s)	$1.014 \times 10^{-5}$	$0.86 \times 10^{-5}$
Surface tension (N/m)	0.021	0.0212
Latent heat (J/kg)	$1167 \times 10^3$	$536 \times 10^3$
Merit number (kg/s <sup>3</sup> )	$4.31 \times 10^{10}$	$3.24 \times 10^{10}$

#### B. PCM Drawer Design

Several key parameters for the drawer design must be carefully considered. They are listed as follows,

- PCM thickness ( $d_{\text{pcm}}$ ): Increasing the bulk PCM thickness can effectively increase the mass ratio, but it will also increase the temperature drop across the PCM.
- Vapor space thickness ( $d_{\text{vc}}$ ): To achieve a higher mass ratio, the space between drawers should be as narrow as possible. However, reducing the vapor space will eventually lead to the problem of the condensate liquid return being hindered by the incoming vapor shear, referred as the "entrainment limit" of a two-phase system.

- Height of drawers ( $H_{pcm}$ ): increasing the height of the PCM drawers would increase the mass ratio and decrease the temperature drop, but it is limited by the capillary pumping pressure of the mesh wire. Since the only possible ground testing orientation is “against gravity” (where liquid returns to the evaporature upwards), the height was severely limited. Based on the wettability test and the capillary limit calculation, the drawer height for aluminum mesh with mesh size 74 microns ( $200 \text{ in}^{-1}$ ) is 3.05 cm.
- Width of drawers ( $W_{pcm}$ ): increasing the width of drawers will only slightly increase the mass ratio since both PCM and structural material masses increase. The width in this calculation is selected to be 40.64 cm (16.0”).

As depicted in Figure 3, the design calculation of the mass ratio and temperature difference across the PCM starts from a single element represented as a half portion of PCM, drawer envelope, wick structure and main body walls. The most critical parameter in this design is the thickness of PCM ( $d_{pcm}$ ). Figure 4 shows the calculation results. As the PCM thickness increases, the mass ratio of a single element will increase substantially while the slope will decrease. Eventually, the mass ratio will reach a constant value of around 0.67. The downside of increasing the PCM thickness is the effect on temperature gradient ( $\Delta T$ ) across PCM. In Figure 4, with a constant heat flux  $500 \text{ W/m}^2$ , the corresponding temperature drop across PCM increases linearly with the PCM thickness. For the avionics box temperature regulation, it is reasonable to limit the maximum temperature below  $45^\circ\text{C}$ . The PCM melting temperature in this system is set to be  $25^\circ\text{C}$ , so the acceptable temperature drop across PCM must be smaller than  $15^\circ\text{C}$ , so the proper PCM thickness is determined to be 1.27 cm. One thing that must be addressed is that the temperature drop of  $15^\circ\text{C}$  only happens when the entire inventory of PCM within the heat exchanger was melted. During the normal operation mode, the temperature drop will be much smaller.

With a PCM thickness of 1.27 cm, the mass ratio is about 0.61. It is possible to achieve a higher mass ratio by further reducing the wall thickness of the main body as well as the drawer enclosure. In this calculation, the wall thickness is 0.5 mm. If the wall thickness can be reduced to 0.4 mm, the mass ratio can increase to 0.70.

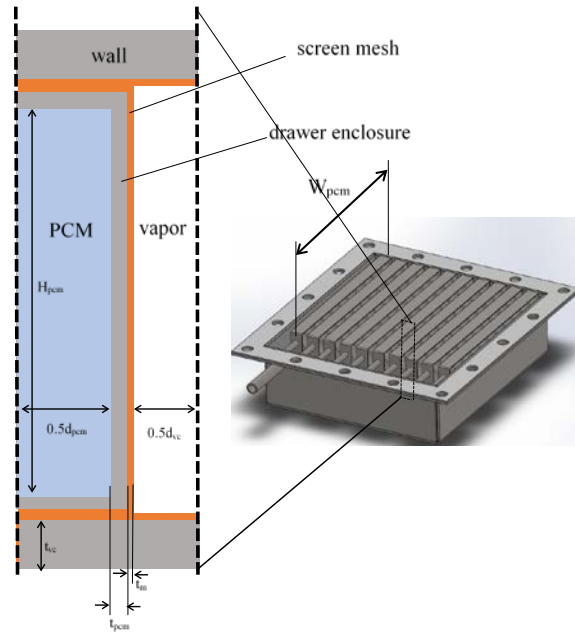


Figure 3. Design model for a single PCM drawer

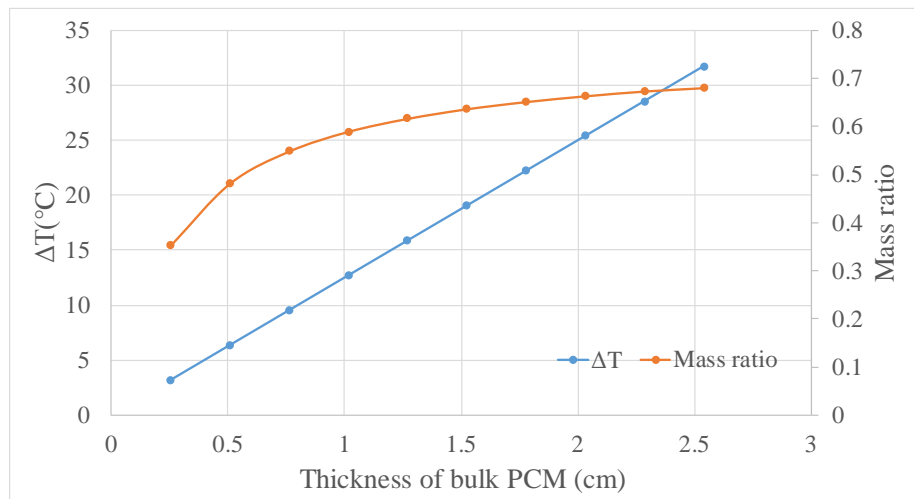


Figure 4. Effect of PCM thickness on mass ratio and temperature gradient across bulk PCM ( $k_{pcm} \sim 0.20 \text{ W/mK}$ )

### C. 1D Transient PCM Phase Change Model

To study the thermal storage capacity of the drawer, a simple 1D transient analytical model to describe PCM melting process is introduced. The model depicted in Figure 5 has the following assumptions:

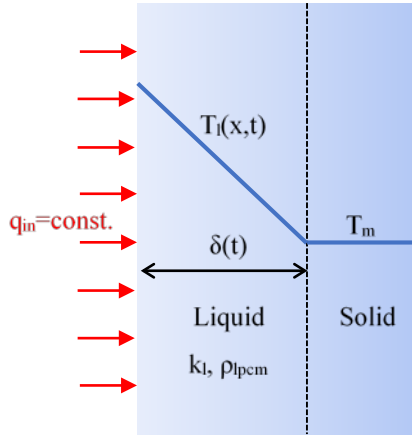


Figure 5. PCM melting theoretical model

- One-dimensional heat transfer
  - Heat flux applied from the left is a constant during the entire phase change process
  - The system is quasi-steady
  - Latent heat based energy storage is much greater than the sensible heat based energy storage. (i.e. Stefan number  $\ll 1$ )
- Under these assumptions, at each time step the temperature profile within the melting region must be linear, which can be expressed mathematically as,

$$T_l(x, t) = a_1(t) + a_2(t)x$$

where  $a_1$  and  $a_2$  are functions of time only.  $a_2$  can be determined easily by applying the constant heat flux boundary from the left.

$$a_2(t) = -\frac{q_{in}}{k_l}$$

To determine  $a_1(t)$ , another boundary condition is applied at the moving solid-liquid interface, that is

$$\text{at } x = \delta(t), T_l = T_m$$

Based on the conservation of energy principle, the interface moving speed can be expressed as follows,

$$(\rho_{lpcm}\lambda_f) \frac{d\delta}{dt} = -k_l \frac{\partial T_l}{\partial x} = q_{in}$$

and the interface location with respect to time can be expressed as,

$$\delta(t) = \frac{q_{in}}{\rho_{lpcm}\lambda_f} t$$

By combining the expressions above, we can derive the temperature profile within the melting region.

$$T_l(x, t) = T_m + \frac{q_{in}^2}{\rho_{lpcm}\lambda_f k_l} t - \frac{q_{in}}{k_l} x$$

With a  $500\text{W/m}^2$  heat input, temperature profiles within a 1.27 cm thick PCM at different time are plotted in Figure 6. At  $t = 500$  s, about 1/3 of PCM is melted and the temperature gradient across PCM is about  $3^\circ\text{C}$ . The heat storage can be calculated by multiplying the latent heat, density, PCM area and the melting region thickness ( $\delta$ ) at a certain time. This model can then be integrated into a thermal-resistance network for the system level temperature analysis.

### IV. Proof-of-concept Prototype Fabrication

ACT designed and fabricated a proof-of-concept prototype based on the mathematical model described above. Dimensions and other specifications of the sub-scale prototype are summarized in Table 2. The following section will summarize the fabrication process.

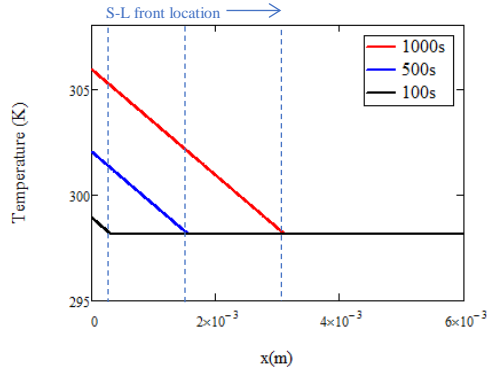


Figure 6. Theoretical temperature profiles and the melting front location at different time with heat flux  $500\text{W/m}^2$

**Table 2. Proof-of-concept prototype specifications**

Specifications	Value
L×W×H	10.9 cm × 15.24 cm × 3.35 cm
PCM thickness	0.635 cm
Gap between PCM drawers	0.32 cm
# of drawers	10
Vapor chamber wall thickness	1.59 mm
PCM drawer wall thickness	0.5 mm
Screen Mesh	74 micron, $d_w=53.34 \mu\text{m}$
Working fluid	Acetone
Structural Material	Aluminum 6061
PCM	PureTemp25 <sup>®</sup> ( $T_m=25^\circ\text{C}$ ) <sup>2</sup>
Capillary limit	70W
Mass ratio (exclude flange)	0.4
Total thermal storage capacity	42kJ

mass of drawers, the envelope wall thickness must be as thin as possible. Nevertheless ultra-thin walls must be completely sealed to prevent PCM leaking into the heat exchanger. Drawer envelopes are fabricated by the electrical discharge machining (EDM) method. After welding the end caps and the fill tube, drawers are charged with the commercially available PCM (PureTemp) by syringe. To accommodate PCM volumetric expansion during phase transition, in liquid state, the amount of PCM charged into each drawer is carefully measured by a digital scale (up to 3-digits accuracy) and make sure that there is no PCM liquid residual inside the fill tube. When the PCM is frozen, it will contract volumetrically by 10%.

To check whether the drawer is leak-tight, drawers after charging are placed into a sealed chamber (e.g. heat exchanger main body) with a small amount of heat applied. The chamber is evacuated and stays in vacuum for a long period. Three pieces of evidence indicate that drawers are completely sealed:

- (1) Pressure within the heat exchanger remains the same during the overnight data collection.
- (2) There is no weight loss after the test.
- (3) No PCM is found outside of the drawers after the test.

The last step of drawer fabrication is screening the drawer with aluminum mesh. The end product shown in Figure 7 has the mass ratio around 0.6.

#### F. Prototype Assembly

After rinsing with acetone, drawers are placed inside the main body. The space between drawers is fixed by a spacer, which is a small piece of aluminum sheet cut with 10 slots. Drawer fill tubes are clamped into the slots as Figure 7 shows. When the drawer is inserted into the main body, the screen mesh are slightly compressed, so it can hold the drawers in position similar to a spring holding a battery in electronic devices. After drawers are fastened, the heat exchanger is closed and sealed. After evacuation and charging with a certain amount of working fluid, the device is ready for the thermal performance test.

#### D. Main Body

The main body of the heat exchanger is fabricated from an aluminum sheet. The sheet is cut into a certain shape via water-jet cutting, then folded into the box. Since the sub-scale prototype will be opened frequently for cleaning and inspection, it is more convenient to couple the top cover and the main body through a flange and sealed with o-rings. The interior surface is covered with aluminum screen mesh. A fill tube is welded on one side of the main body for working fluid charging.

#### E. Drawer Fabrication

Drawer fabrication is challenging, mainly due to the trade-off between the mass reduction and seal integrity. To minimize the

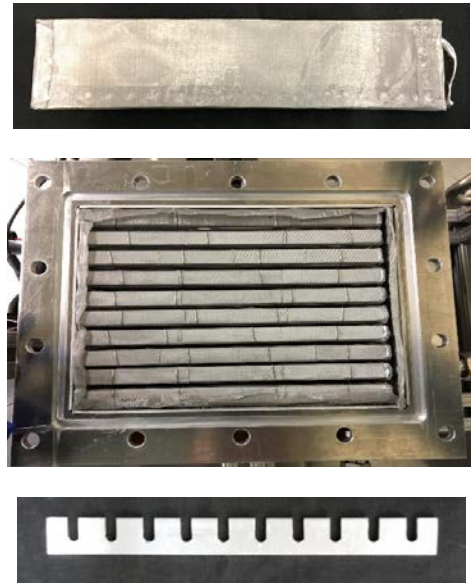


**Figure 7. The proof-of concept PCM heat exchanger (Upper: PCM drawer fabricated by EDM method. Middle: heat exchanger contains with 10 drawers. Lower: drawers spacer).**

## V. Thermal Performance Test

To test the thermal performance of the PCM heat exchanger, an experimental apparatus is designed and built. The test system is composed of the following components:

- Chiller block: a 1.27 cm thick chiller block is mounted on the top cover of the heat exchanger. Cooling is provided by liquid nitrogen (LN).
- Heat source: heat is applied from the bottom of the heat exchanger through a heater block, which is an aluminum block with cartridge heaters. In this test, the maximum heat input is 70W.
- The bell jar system: tests are performed within the bell jar under vacuum for two reasons, (1) to minimize air leaking into the heat exchanger through the flange coupling and (2) to reduce heat leaking from the heat exchanger surface to the environment.

T-type thermocouples are used for temperature measurement. The probes are attached as follows: eight to the top and bottom plates, four probes to the side of the heat exchanger, and two in the chiller block inlet and outlet. One thermocouple is attached to the heater block and one is placed inside the bell jar to track the ambient temperature. One thermowell is extruded from the chiller plate into the heat exchanger to measure the interior temperature. The saturation vapor pressure within the heat exchanger is measured by a high-accuracy pressure transducer attached to the side of the main body.

The following 3 tests are performed to study the developed PCM heat exchanger thermal characteristics.

- (1) **Dry mode:** The purpose of the test is to set up a baseline for comparison and also simulate the worst case in an operation. This test is performed while the heat exchanger has no working fluid inside.
- (2) **Heat exchanger (HX) mode:** In this test, the heat exchanger is charged with 5ml of working fluid (acetone). The thermal performance of the module with PCM in solid state/liquid state will be studied by maintaining the saturated vapor temperature below/above the melting point of the PCM through controlling the LN flow rate. Under different heat inputs, the steady-state temperature distributions are recorded and the effective thermal conductances are analyzed. All tests are conducted in both gravity-aided and against-gravity orientations, which can be performed by switching the locations of the heater block and the chiller block.
- (3) **Dual mode:** The HX-capacitor dual mode is the highlight of the developed device. This test is to simulate a generic situation when the environmental temperature or the heat load abruptly changes during a space mission. The developed device is expected to minimize the effect of the environment temperature fluctuation and the heat source temperature. The test procedure is depicted at Figure 9. Initially, the system temperature is maintained below the PCM melting point. At  $t=0s$ , heat (15W) is applied to the evaporator with the condenser thermally-insulated. The system temperature increases with time until it reaches the PCM melting point and the system enters the heat storage period, which can be identified by the temperature flatness. When all PCM is melted, temperature raises again. The LN valve is then opened and the system is being cooled. The temperature is maintained at a high level for a certain period, then the heater is suddenly turned-off. The temperature quickly drops and the system enters the heat releasing period. The total thermal storage capacity can be estimated by multiplying the heat input with the temperature flatness period. The test is performed in both gravity-aid and against-gravity orientation.

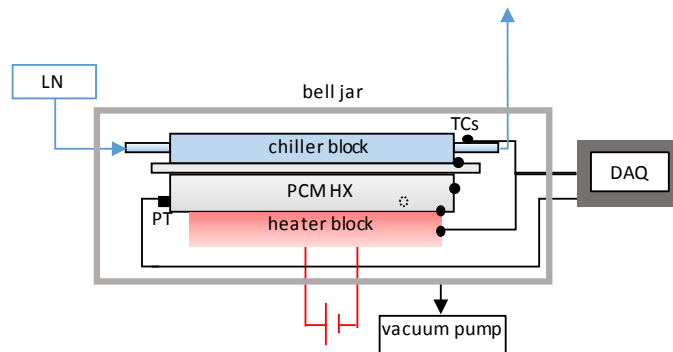


Figure 8. Thermal performance test apparatus

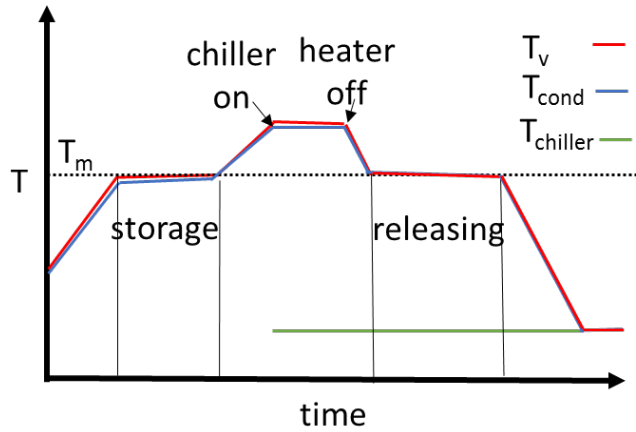


Figure 9. Test procedure for the dual mode test

## VI. Results and Discussion

### A. Heat Exchanger Mode

Temperature profiles with different heat inputs of the dry test and heat exchanger test are plotted in Figure 10. In the dry test, the side wall temperature is maintained at 15°C. As figure in left shows, when  $Q=60\text{W}$ , the temperature drop ( $\Delta T$ ) across the evaporator and the condenser is around 15°C, so the total thermal resistance is 0.25K/W. With a small amount of working fluid,  $\Delta T$  can be reduced to 8°C with the same heat input and the corresponding thermal resistance reduces to 0.13K/W. The heat transfer capability of the developed device can be easily identified by the plotting thermal resistance under various conditions in Figure 11. Due to the additional heat transfer “short cut” created by the two-phase working fluid, the thermal resistance for heat exchanger mode can be reduced by 40%. In addition, Figure 11 shows that the thermal resistance under gravity-aided and against-gravity orientation nearly identical, which indicates that the developed two-phase heat exchanger can operate in micro-gravity.

The total thermal resistance for heat exchanger mode and dry mode can be predicted based on the thermal resistance networks depicted in Figure 12. For the dry mode, it can be shown that the dominant thermal path is the in-plane heat conduction through drawer thin walls ( $R_{s2}$ ) and for the heat exchanger mode, the dominant thermal path changes to the two-phase heat transfer. The two-phase heat transfer thermal resistance consists of the conduction through the saturated screen mesh, nucleate boiling and film-wise condensation. For the saturated wick structure, the effective thermal resistance can be evaluated by the following equations<sup>3</sup>

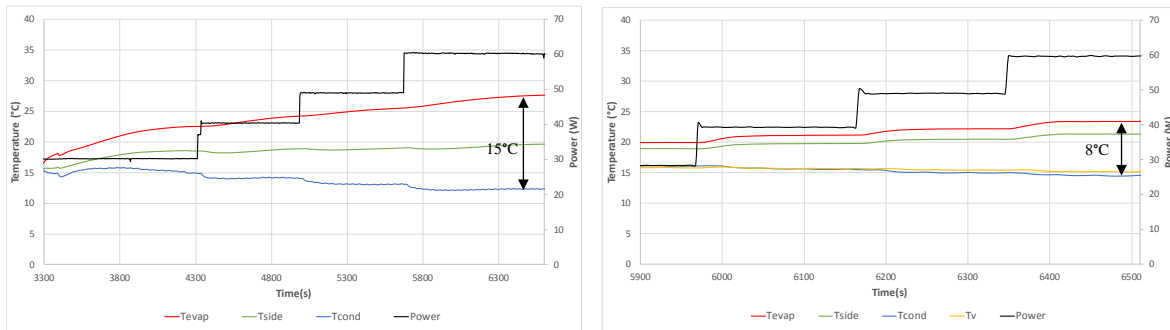


Figure 10. Temperature profiles of the PCM-based heat exchanger (left: dry mode; right: with working fluid)

$$k_{eff} = \frac{k_f[(k_f + k_m) - (1 - \varepsilon_m)(k_f - k_m)]}{[(k_f + k_m) - (1 - \varepsilon_m)(k_f - k_m)]}$$

$$R_m = \frac{t_m}{A_m k_{eff}}$$

The evaporative thermal resistance was determined from the Rohsenow's boiling correlation<sup>4</sup>, that is

$$\Delta T_e = \frac{\lambda}{C_{p,l}} Pr^n C_{sf} \left[ \frac{q''}{\mu_l \lambda} \left( \frac{\sigma}{g(\rho_l - \rho_v)} \right)^{1/2} \right]^{1/3}$$

and

$$R_{evap} = \frac{\Delta T_e}{A_{evap} q''}$$

Two coefficients  $n$  and  $C_{sf}$  are 0.17 and 0.0130. For the condensation, the thermal resistance can be evaluated by the film-wise condensation model.

$$\Delta T_c = \left[ \frac{4q''^4 \mu_l d_v / 2}{0.791 \lambda \rho_l (\rho_l - \rho_v) g k_f^3} \right]^{1/3}$$

Other components of the thermal resistance are listed in Table 4. The total thermal resistance is calculated by the parallel heat conduction model and plotted as the solid lines in Figure 11. In general, the predicted value has a good agreement with the experimental data. Furthermore, the thermal resistance is generally lower when the enclosed PCM is in the liquid state.

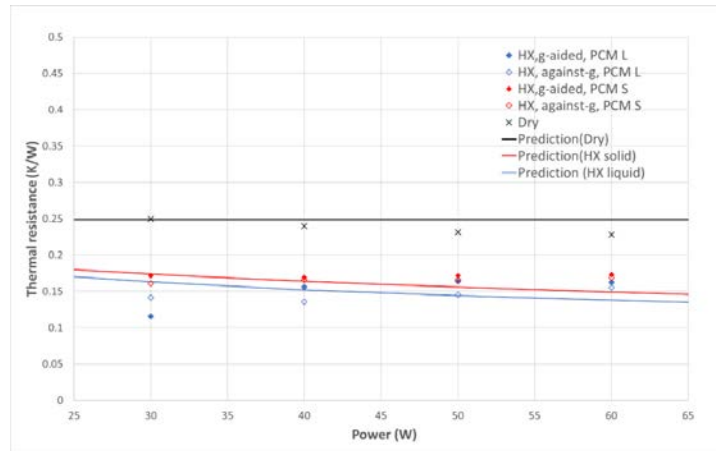


**Figure 11. Thermal resistance of the proof-of-concept prototype under various conditions (lines: prediction, dots: test results)**

**Table 3. Predicted thermal resistances breakdown for the proof-of-concept prototype (for a single drawer)**

Item	Description	Predicted Value (K/W)	Notes
$R_{s1}$	Conduction through top and bottom	0.01	-
$R_c$	Total contact resistance	1.67	Include mesh-mesh and mesh-solid contact
$R_{s2}$	Conduction through drawer wall	2.45	-
$R_{pcm1}$	Conduction through bulk PCM (lateral)	326.21	-
$R_m$	Resistance of saturated screen	0.15	Estimated from screen mesh effective thermal conductivity formula <sup>3</sup>

## B. Dual Mode

To demonstrate the thermal storage capacity of the developed two-phase system, ACT performs the dual mode test and one of the test result is shown in Figure 13. The initial temperature of the system is controlled at 5°C. At  $t=1000s$ , 15W of heat is applied to the system from the heater block and the coolant (LN) valve is simultaneously closed. This stage can be regarded as the spacecraft launching stage, when the wasted heat generated from electronics cannot be dissipated by the heat rejection system. The system temperature starts increasing. As the temperature reaches approximately 27°C (slightly above the PCM melting point), the system enters the heat storage mode. As the figure indicates, the developed device has an outstanding thermal storage performance, which can be identified from the sharp temperature curvature change. During the heat storage period, the saturated vapor temperature is higher than the PCM melting point, and the saturated vapor condenses on the drawer surface and deposits its latent heat into the bulk PCM. Due to the large amount of PCM within the main body, the evaporator temperature can be maintained below 30°C for 5000 seconds. At  $t=10000s$ , another temperature curvature change can be identified, which indicates that the melting process is complete. Since the device is capable of storing 15W of heat for 5000 seconds, the overall thermal storage capacity is 75kJ.

The LN valve was opened at  $t=14500s$ . From 15000s to 19000s, the device demonstrates its two-phase heat transfer capability at high working temperature. With 15W of heat input,  $\Delta T$  from evaporator to condenser is around 2.5°C. At  $t=19000s$ , the heater is suddenly turned-off, and the system temperature drops dramatically. The system enters the heat releasing mode. The intention of this period is to simulate a generic situation which the spacecraft is orbiting in space with a low sink temperature and the heat load from the internal loop decreases. As Figure 13 shows, PCM starts freezing at  $t=20500s$ , which prevent the system temperature from dropping for more than an hour. In the heat releasing period, heat stored within the PCM is released to the saturated vapor. To be noted is that the test was conducted in the against-gravity orientation, which indicates that the fine screen mesh in this device can successfully transport working fluid between the evaporator, condenser and drawer surfaces regardless the orientation.

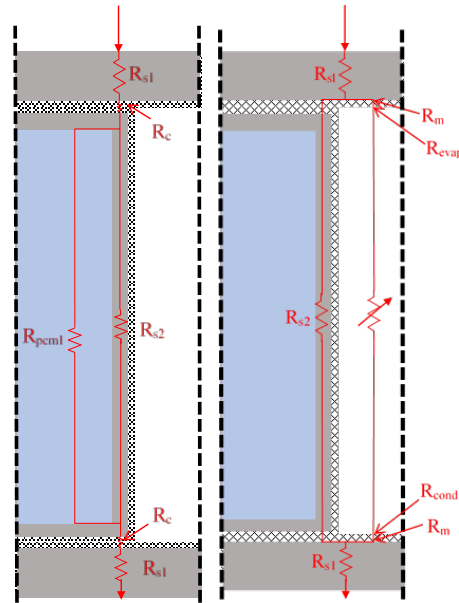


Figure 12. Thermal resistance network for different mode (a) dry mode (b) heat exchanger mode

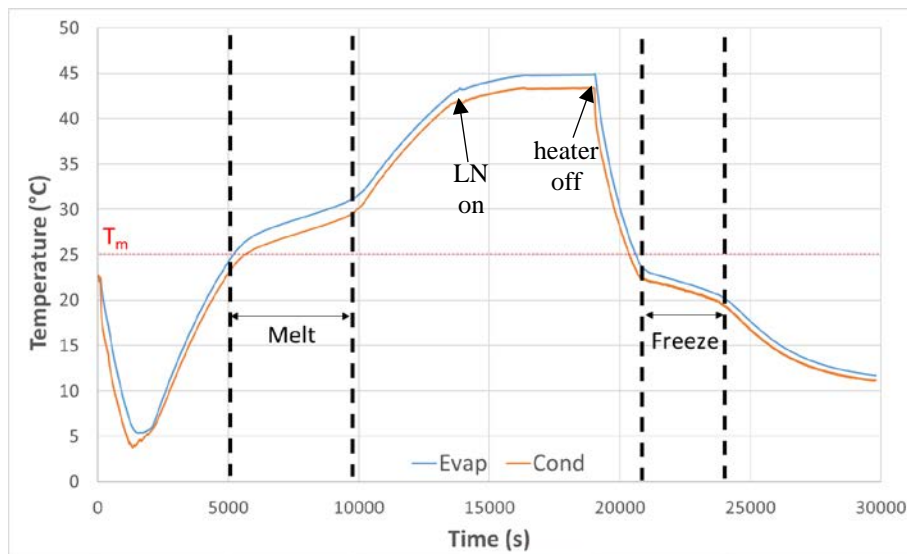


Figure 13. Dual mode test result under against-gravity orientation

### C. Comparison with Standard Heat Capacitors

By replacing the solid thermal conductive material with the two-phase working fluid, a significant amount of mass can be saved. Take the proof-of-concept prototype for example, if all the vapor space is occupied by aluminum alloy, the total mass will increase from 0.6 kg to 1.3 kg. In other words, with the same thermal storage capacity, the weight of developed two-phase device is only 46% of the conventional PCM heat sink with aluminum fin structure.

## VII. Conclusion

An innovative two-phase heat exchanger with multiple PCM drawers was designed and fabricated by Advanced Cooling Technologies, Inc. Unlike conventional PCM-based heat exchangers, heat is distributed to the PCM by a two-phase working fluid. PCM-filled drawers are inserted into the vapor space to store the excessive heat. By replacing the solid heat conduction material within traditional thermal capacitors with the two-phase working fluid, the developed thermal device is expected to have both high mass ratio and low thermal resistance. In addition, under different environmental conditions, the developed device can change its operation mode from a two-phase heat exchanger to a thermal capacitor and reduce the effect of environment temperature fluctuations substantially. This paper presents the PCM heat exchanger design process, including material and working fluid selection, wick structure and geometry considerations, and a 1D PCM phase transition analytical model. In addition, a proof-of-concept aluminum-acetone prototype was designed, fabricated, and tested in a bench-top thermal performance test system. Through the trade study, the developed system can potentially achieve a high PCM/total mass ratio 0.7. Through experimental study, the developed proof-of-concept prototype demonstrate the following thermal performance

(1) the overall thermal resistance can be reduced by 40% through two-phase heat transfer

(2) the small-scale prototype (10 cm by 15cm) can store 75kJ of heat

(3) the developed system can successfully operate under the most conservative orientation which is the “against gravity”, where the heat is applied at the top of the heat exchanger.

The developed PCM-based two-phase heat exchanger is capable of transferring heat when sink temperature is low and storing heat when sink temperature is high, in both cases with minimum thermal resistance.

## Acknowledgements

This project is funded by NASA Marshall Space Flight Center under a SBIR Phase II program (Contract NNX15CM02C). The technical monitor is Brian O’Conner. Special appreciation to Zach Bitner for the technical efforts as well as Tim Wagner and Andy Huber for their support in the PCM drawer fabrication process.

## References

- <sup>1</sup> Yun, J., Tarau, C., & Van Velson, N. (2016). Status of the Development of a Vapor Chamber with Phase Change Material-Based Wick Structure. *46th International Conference on Environmental Systems*. Vienna.
- <sup>2</sup> Entropy Solutions, LLC. (2017). *PureTemp 25 technical data sheet*. Retrieved from PureTemp technical data sheets: <http://www.puretemp.com/stories/puretemp-25-tds>
- <sup>3</sup> Chi, W. *Heat pipe Theory and Practice*, McGraw-Hill, New York, 1976.
- <sup>4</sup> Rosenhow, M., A Method for Correlating Heat Transfer Data for Surface Boiling of Fluids. *ASME J. Heat Transfer* **74**, 969-976, 1952.